

# Searching for the First Galaxies through Gravitational Lenses

Daniel Schaerer<sup>1,2</sup>  
 Roser Pelló<sup>2</sup>  
 Johan Richard<sup>2,5</sup>  
 Eiichi Egami<sup>3</sup>  
 Angela Hempel<sup>1</sup>  
 Jean-François Le Borgne<sup>2</sup>  
 Jean-Paul Kneib<sup>4,5</sup>  
 Michael Wise<sup>6</sup>  
 Frédéric Boone<sup>7</sup>  
 Françoise Combes<sup>7</sup>

<sup>1</sup> Geneva Observatory, Sauverny, Switzerland

<sup>2</sup> Observatoire Midi-Pyrénées, Laboratoire d'Astrophysique, Toulouse, France

<sup>3</sup> Steward Observatory, University of Arizona, Tucson, Arizona, USA

<sup>4</sup> OAMP, Laboratoire d'Astrophysique de Marseille, Marseille, France

<sup>5</sup> Caltech Astronomy, Pasadena, California, USA,

<sup>6</sup> Astronomical Institute Anton Pannekoek, Amsterdam, the Netherlands

<sup>7</sup> LERMA, Observatoire de Paris, France

Observing the first galaxies formed during the reionisation epoch, i.e. approximately within the first billion years after the Big Bang, remains one of the challenges of contemporary astrophysics. Several efforts are being undertaken to search for such remote objects. Combining the near-IR imaging power of the VLT and the natural effect of strong gravitational lensing our pilot programme has allowed us to identify several galaxy candidates at redshift  $6 \lesssim z \lesssim 10$ . The properties of these objects and the resulting constraints on the star-formation rate density at high redshift are discussed. Finally we present the status of follow-up observations (ISAAC spectroscopy, HST and Spitzer imaging) and discuss future developments.

Like the explorers of seas and continents in the past centuries, astronomers keep pushing the observational frontiers of the Universe with their telescopes thereby tracing back the history of stars and galaxies since their birth. Just a few years ago, in 2002, the most distant galaxy known was a faint unobscured object called HCM 6A at redshift  $z = 6.56$  discovered thanks to the natural effect of

gravitational lensing provided by a foreground cluster of galaxies, which magnifies the light of this distant background object (Hu et al. 2002). A few quasars at similar distances had also been discovered, pushing our 'observational horizon' already back in time to a little less than one billion years after the Big Bang, close to the end of cosmic reionisation. However, evidence from cosmic microwave background polarisation measurements and other arguments indicate that star formation in galaxies must have occurred even earlier.

Since the early nineties, the so-called Lyman break or 'dropout' technique had established itself as a simple and successful method to identify distant galaxies through the use of broadband photometry. Furthermore, sensitive infrared instruments were now available on the large ground-based telescopes, able in principle to detect protogalaxies out to even higher redshifts. Given these advances, we started a few years ago a pilot project with the aim of finding star-forming galaxies at redshifts beyond 6–6.5 using lensing clusters as gravitational telescopes, a well-established technique nowadays. This project is mainly based on ISAAC and FORS2 data plus additional observations obtained at CFHT and HST.

## Observations

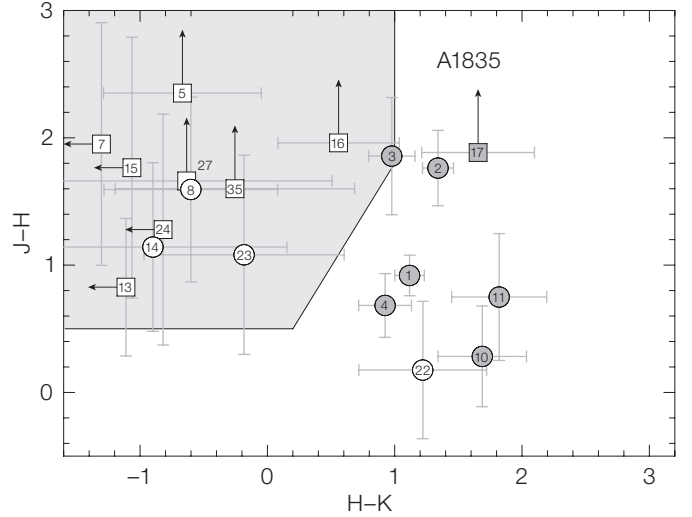
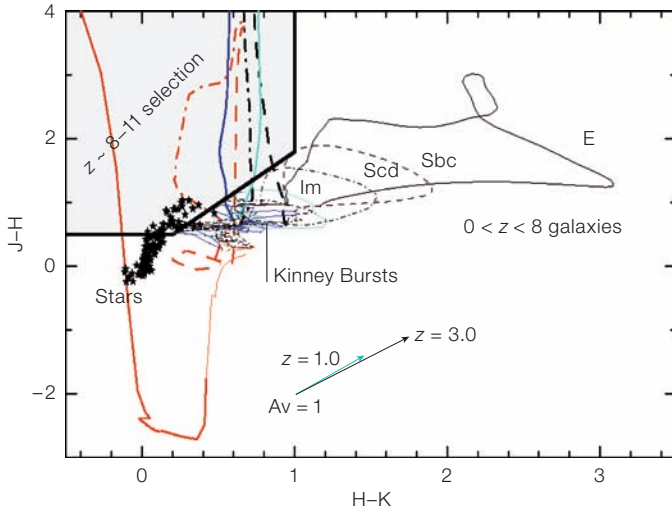
Focussing on two well-known gravitational lensing clusters, Abell 1835 and AC114, we obtained deep near-IR images in the SZ, J, H, and Ks bands with ISAAC and an additional z-band image with FORS2. These deep images, reaching e.g. a  $1 \sigma$  depth of 26.1 in  $H_{AB}$ , were then used to search for objects which are detected at least in two near-IR bands, which show a blue near-IR colour, and which are undetected (i.e. 'drop-outs') in all optical bands. These criteria are optimised to select high-redshift ( $z > 6$ ) objects with intrinsically blue UV-restframe spectra, i.e. very distant starburst galaxies, and to avoid contamination from intrinsically faint and red cool stars. Different combinations of colour-colour plots allow a crude classification into several redshift bins. An example of such a diagram, showing the expected location of  $z \sim 8$ –11 galax-

ies and of candidates found behind Abell 1835 is shown in Figure 1. A complete report is given in Richard et al. (2006).

## High-z galaxy candidates and the cosmic star formation density during reionisation

In spring 2003 the analysis of the candidates behind Abell 1835 yielded an intriguing, strongly lensed object whose spectral energy distribution was compatible with that of a galaxy at  $z \sim 9$ –11. During our first spectroscopic follow-up run with ISAAC in summer 2003 we were able to secure J-band long-slit spectroscopy centred at this position under excellent seeing conditions. Interestingly, careful data reduction revealed at this location the presence of a single faint emission line detected at  $\sim 4$ –8  $\sigma$  (depending on the integration aperture and stacking procedure), which if interpreted as Ly $\alpha$  would indicate  $z = 10.0$ ! The report of these findings was published in Pelló et al. (2004a).

*What is the status of this fairly unique candidate?* Weatherley et al. (2004) have questioned the reality of the emission line. However, their negative result could be due to the combination of two factors: an error in our absolute wavelength calibration discovered later, and their spectroscopic data reduction technique, where the information is only preserved at the original (wrong) wavelength position and smeared elsewhere (see Pelló et al. 2004b). On the imaging side, deep V-band observations with FORS2 (Lehnert et al. 2005) have confirmed its optical non-detection. Our ISAAC H-band images have been reanalysed by several groups using different methods (Bremer et al. 2005, Smith et al. 2006) yielding measurements compatible with ours typically within  $1 \sigma$ . Surprisingly however, this object remained undetected in a deeper NIRI/GEMINI H-band image taken approximately 15 months after our ISAAC image (Bremer et al. 2005). In spring 2004 we obtained two SZ ( $\sim 1.06 \mu\text{m}$ ) images with ISAAC, where this object is again detected (see Pelló et al. 2005). Taken together these spectroscopic and photometric detections, albeit individually of relatively low significance, indicate that this source is most likely not a spu-



rious, but an intrinsically variable object, as discussed in Richard et al. (2006). Therefore, its nature and precise redshift remain puzzling, and we exclude this object from our list of high- $z$  candidates, which we will discuss now.

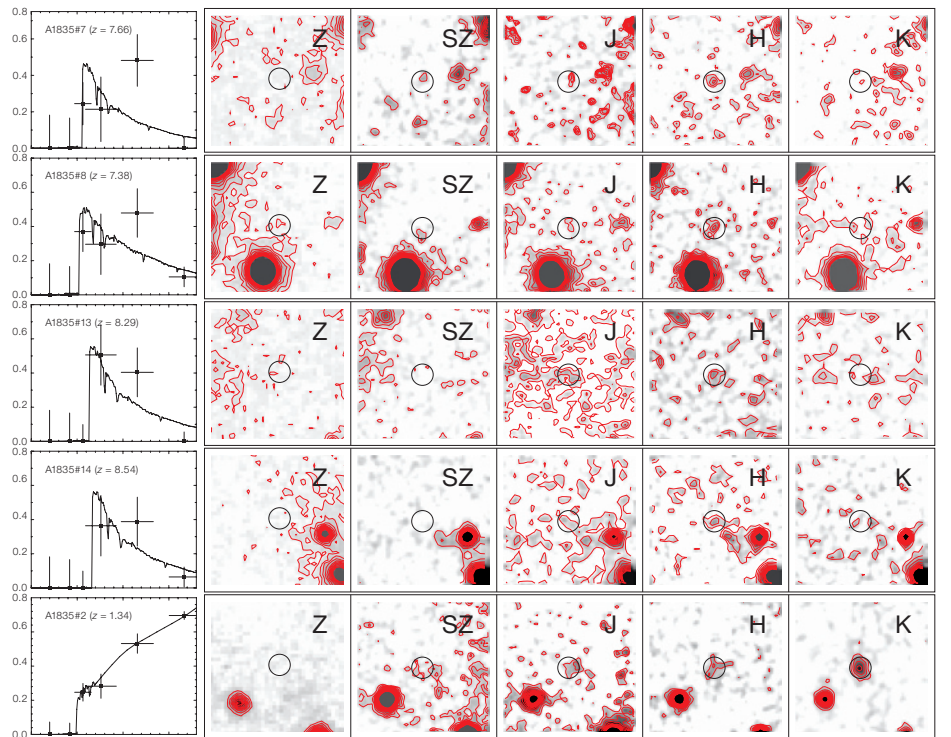
Applying the above selection criteria to the observations of the two lensing clusters has yielded 13 candidates whose spectral energy distributions (SEDs) are compatible with those of star-forming galaxies at  $z \geq 6$  (see Richard et al. 2006). Images and the SEDs of some of them are shown in Figure 2 for illustration. The typical lensing magnification reaches from 1.5 to 10, with an average of  $\sim 6$ , i.e. nearly two magnitudes. Their star formation rate, as estimated from the UV restframe luminosity, is typically between 4 and  $20 M_{\odot} \text{ yr}^{-1}$  after correcting for lensing.

We have used these data to attempt to constrain for the first time the density of star-forming galaxies present at  $6 \leq z \leq 10$  using lensing clusters. After taking into account the detailed lensing geometry, sample incompleteness, and correcting for false-positive detections we have constructed a luminosity function (LF) of these candidates assuming a fixed slope taken from observations at  $z \sim 3$ . Within the errors the resulting LF is compatible with that of  $z \sim 3$  Lyman break galaxies. At low luminosities it is also compatible with the LF derived by Bouwens and collaborators for their sample of  $z \sim 6$  candidates in the Hubble Ultra Deep Field (UDF) and related fields. However, the turnover

observed by these authors towards the bright end relative to the  $z \sim 3$  LF is not observed in our sample. Finally, from the LF we determine the UV star formation rate (SFR) density at  $z \sim 6-10$ , shown in Figure 3. Our values indicate a similar SFR density as between  $z \sim 3$  to 6, in contrast to the drop found from the deep NICMOS fields. Further observations are required to fully understand these differences. Taken at face value, this relatively high SFR density is in good agreement e.g. with the recent hydrodynamical mod-

**Figure 1 (Above):** Colour-colour diagrams (in the Vega system) showing (Left) the location for different objects over the interval  $z \sim 0$  to 11 and our selection region for galaxies in the  $z \sim 8-11$  domain and (Right) the location of the individual optical dropouts detected in Abell 1835. Circles and squares correspond to high- $z$  candidates detected in three and two filters respectively. Optical dropouts fulfilling the ERO definition are shown in grey.

**Figure 2 (Below):** Close-up of four high- $z$  candidates in Abell 1835, showing the objects and their surrounding  $10 \times 10$  arcsec fields in optical ( $z$ ) and near-IR bands (SZ, J, H, and Ks) as well as their SED. For comparison the image and SED of an intermediate redshift ERO is also shown at the bottom.



els of Nagamine et al. (2005), with the re-ionisation models of Choudhury and Ferrara (2005), and also with the SFR density inferred from the past star formation history of observed  $z \sim 6$  galaxies (e.g. Eyles et al. 2006).

### Follow-up observations

Compared to the data set just described several additional observations were secured on these clusters in the meantime. For example, deep  $z$ -band images of both clusters were obtained with the ACS camera onboard HST. These observations confirm that the vast majority (all except one of the above 13) of our high- $z$  candidates are optical dropouts as expected, remaining undetected down to a  $1\sigma$  limiting magnitude of  $28\text{--}28.3\text{ mag}_{AB}$  (Hempel et al. 2006). In collaboration with Eiichi Egami we have also access to IRAC/Spitzer GTO images at 3.6, 4.5, 5.8 and  $8.0\text{ }\mu\text{m}$  of large sample of lensing clusters including Abell 1835 and AC114. Again, none of our high-redshift galaxy candidates are detected. This is easily understood, since extrapolation of their intrinsically blue SED to IRAC wavelengths shows that their expected fluxes fall below the Spitzer sensitivity. It implies that these objects do not host ‘old’ stellar populations with strong Balmer breaks, and that they are not affected by significant extinction. A more detailed account of these observations will be presented elsewhere. For comparison a brighter lensed galaxy at  $z \sim 7$  has been detected earlier by Spitzer (Egami et al. 2005).

In parallel several attempts were made to detect emission lines from selected candidates using near-IR long-slit spectroscopy with ISAAC on the VLT. See Pelló et al. (2005) for a preliminary report. Presently such observations are tedious, fairly time-consuming, and require excellent seeing conditions. Indeed, given the faintness of the expected lines, the strong IR background, and the need for the highest spectral resolution possible to minimise the impact of the numerous sky lines, a ‘scan’ of the entire  $J$ -band at  $R \sim 3000$  for example requires five settings and a total of  $\sim 10\text{ ksec}$  to detect an unresolved line of  $(6\text{--}8) \times 10^{-18}\text{ erg s}^{-1}\text{ cm}^{-2}$  flux at  $5\sigma$  with ISAAC.

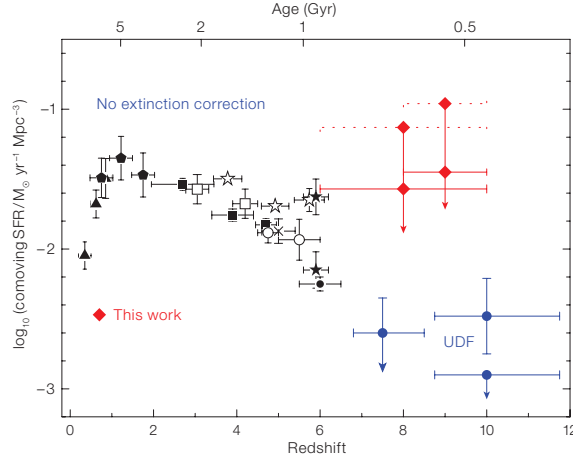


**Figure 3:** Evolution of the comoving Star-Formation Rate (SFR) density as a function of redshift including a compilation of results at  $z \lesssim 6$ , our estimates obtained from both clusters for the redshift ranges  $[6\text{--}10]$  and  $[8\text{--}10]$  and the values derived by Bouwens and collaborators from the Hubble Ultra-Deep Field (labelled ‘UDF’; Bouwens et al. 2004, ApJ 616, L79 and 2005, ApJ 624, L5). Red solid lines: SFR density obtained from integrating the LF of our first category candidates down to  $L_{1500} = 0.3 L^*_{z=3}$ ; red dotted lines: same as red solid lines but including also second-category candidates with a detection threshold of  $< 2.5\sigma$  in  $H$ .

One or more emission lines could be detected in few objects, as shown in Figure 4. For example, one of our secondary targets turned out to be a very faint  $z = 1.68$  emission line galaxy. Other lines are clearly identified as the  $[\text{OII}] \lambda 3727, 3729$  doublet from an intermediate redshift galaxy. Finally several objects show a single emission line, which – if identified as  $\text{Ly}\alpha$  – yields a redshift compatible with the (high) estimated photometric redshift. However, in none of these cases a clear asymmetry of the line, as typical for  $\text{Ly}\alpha$  from lower- $z$  starbursts, was found. Searches for additional lines in these objects (e.g.  $\text{CIV} \lambda 1550$  or  $\text{HeII} \lambda 1640$  if at high  $z$ , or for  $[\text{OIII}] \lambda 5007$  or  $\text{H}\alpha$  if at low  $z$ ) have so far been negative. Therefore the redshifts of these objects are currently difficult to establish, but high- $z$  cannot be excluded on the present grounds. Forthcoming, more efficient near-IR spectrographs should allow a significant breakthrough in this field.

### Spin-off projects on EROs and dusty intermediate- $z$ galaxies

Our search for optical dropout galaxies behind lensing clusters yields also other interesting objects, such as extremely red objects (EROs; see Richard et al. 2006). In contrast to the high- $z$  candidates most of them are detected by IRAC/Spitzer. These objects, most likely all at intermediate redshift ( $z \sim 1\text{--}3$ ), turn out to have similar properties as e.g. faint IRAC selected EROs in the Hubble UDF, other related objects such as the putative post-starburst  $z \sim 16.5$  galaxy of Mobasher et al. 2005, and some sub-mm galaxies

(see Hempel et al. 2006). Spectroscopic observations with FORS2 and X-ray Chandra observations are also being secured to clarify the redshift and nature of these interesting optical dropout objects.

### Future

With our pilot programme it has been possible to find several very high redshift candidate galaxies by combining the power of strong gravitational lensing with the large collecting area of the VLT. However, differences with other studies based on deep blank fields are found, and already differences between our two clusters indicate that these could at least partly be due to field-to-field variance. Given the relatively low S/N ratio of the high- $z$  candidates and the large correction factors applied to this sample, it is of great interest to increase the number of lensing clusters observed with this technique.

Furthermore, rapidly upcoming new spectrographs such as the second-generation near-IR VLT instruments XShooter and KMOS, the EMIR spectrograph on the Spanish GRANTECAN telescope and others will provide a huge efficiency gain for spectroscopic follow-up of faint candidate sources, thanks to their increased spectral coverage and multi-object capabilities. Observations at longer wavelengths, e.g. with HERSCHEL, APEX and later ALMA, are also planned to search for possible dust emission in such high- $z$  galaxies and to characterise more completely other populations of faint optical dropout galaxies. Finally the JWST and



ELTs will obviously be powerful machines to study the first galaxies. Large territories remain unexplored in the early Universe!

## References

- Bremer M. et al. 2004, ApJ 615, L1  
 Choudhury T. R. and Ferrara A. 2005, MNRAS 361, 577  
 Egami E. et al. 2005, ApJ 618, L5  
 Eyles L. et al. 2006, MNRAS, submitted, astro-ph/0607306  
 Hempel A. et al. 2006, A&A, submitted  
 Hu E. et al. 2002, ApJ 568, L75  
 Lehnert M. et al. 2005, ApJ 624, 80  
 Mobasher B. et al. 2005, ApJ 635, 832  
 Nagamine K. et al. 2005, New Astronomy Reviews 50, 29  
 Pelló R. et al. 2004a, A&A 416, L35  
 Pelló R. et al. 2004b, astro-ph/0407194  
 Pelló R. et al. 2005, IAU Symp. 225, 373  
 Richard J. et al. 2006, A&A, in press, astro-ph/0606134  
 Smith G. P. et al. 2006, ApJ 636, 575  
 Weatherley S. J. et al. 2004, A&A 428, L29

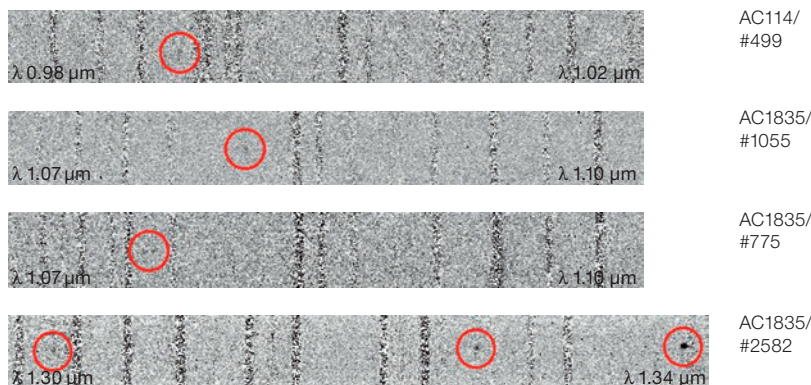


Figure 4: Sky-subtracted 2D ISAAC spectra showing examples of objects with emission line detections marked by red circles in the J band. From top to bottom: A  $z = 7.17$  candidate in AC114, a  $z = 7.89$  candidate in Abell 1835, an intermediate- $z$  galaxy identified by its [OII]  $\lambda 3727, 3729$  doublet, and the  $z = 1.68$  emission line galaxy discovered by Richard et al. (2003, A&A 412, L57). The black vertical lines correspond to sky lines.

## VLT Images of a Disintegrating Comet

On the night of 23 to 24 April, the VLT observed fragment B of the comet Schwassmann-Wachmann 3 that had split a few days earlier. The ESO astronomers were surprised to discover that the piece just ejected by fragment B was splitting again. Five other mini-comets were also visible. The comet thus seems doomed to disintegrate but the question remains in how long a time.

Comet 73P/Schwassmann-Wachmann 3 (SW 3) revolves around the Sun in about 5.4 years, in a very elongated orbit that brings it from inside of the Earth's orbit to the neighbourhood of Jupiter. In 1995, when it was coming 'close' to the Earth, it underwent a dramatic and completely unexpected thousandfold brightening. Observations in 1996, with ESO's NTT and 3.6-m showed that this was due to the fact that the comet had split into three distinct pieces. Later, in December 1996, two more fragments were discovered. At the last comeback (in 2001), of these five fragments only three were still seen, the fragments C (the largest one), B and E. No new fragmentation happened during this approach, apparently.

Things were different this time, when the comet again moved towards its closest approach to the Sun, and to the Earth. Early in March,

seven fragments were observed, the brightest (fragment C) being magnitude 12, while fragment B was 10 times fainter still. In the course of 6 March new fragments were seen.

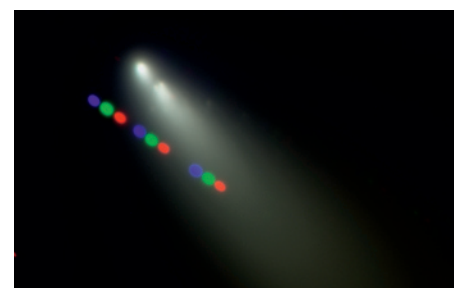
Early in April, fragment B went into outburst, brightening by a factor 10 and on 7 April, six new fragments were discovered, confirming the high degree of fragmentation of the comet. On 12 April, fragment B was as bright as the main fragment C, with a magnitude around 9. Fragment B seemed to have fragmented again, bringing the total of fragments close to 40, some being most probably very small, boulder-sized objects with irregular and short-lived activity.

The new observations reveal that this new small fragment has split again. The image clearly reveals that below the main B fragment, there is a small fragment that is divided in two and a careful analysis reveals five more tiny fragments almost aligned. Thus, this image alone shows at least seven fragments. The comet has thus produced a whole set of mini-comets. Will this process continue? Will the comet finally totally disintegrate? Further observations are planned.

The observations reported here were made with FORS1 on the VLT. The fragment was

observed in four bands (*B*, *V*, *R*, and *I*) for a total of 30 minutes by Emmanuel Jehin, Olivier Hainaut, Michelle Doherty, and Christian Herrera, all from ESO. The astronomers had the telescope track the comet, which explains why the stars appear as trails of coloured dots, each colour corresponding to the order in which the observations were done in the various filters. At the time of the observations, the comet was 26.6 million km away from the Earth, in the constellation Corona Borealis. The final processing of the image was done by Hans Hermann Heyer and Olivia Blanchemain (both ESO).

(From ESO Press Photo 15/06)



Broken fragments of comet SW-3.